

## Structure–Transfection Activity Studies of Novel Cationic Cholesterol-Based Amphiphiles

Molinda D. Kearns, Addai-Mensah Donkor, and Michalak Savva\*

*Division of Pharmaceutical Sciences, Arnold & Marie Schwartz College of Pharmacy and Health Sciences, Long Island University, Brooklyn, New York 11201*

Received September 26, 2007; Revised Manuscript Received November 8, 2007; Accepted November 13, 2007

**Abstract:** Inclusion of DOPE in lipoplex formulations has hampered the establishment of a correlation between cationic lipid structure, biological specificity, and transfection activity, simply because the presence of a helper lipid not only alters the physicochemical properties of the lipoplex but also modifies cell surface specific interactions during the process of transfection. To this end, four cationic cholesterol-based derivatives were synthesized by systematically varying the methylation of the polar headgroup, after which the physicochemical properties, in the absence of DOPE and serum, were correlated with their transfection activity and interaction with cell membranes. It was found that only the primary and secondary amine derivatives, AC-Chol and MC-Chol, respectively, are able to mediate in vitro cell transfection. These results were consistent with fusion experiments and cell internalization studies which illustrated that although cell surface binding occurs for all of the cationic lipids, only the active analogues were able to gain entry into the cytosol. Given the minute differences in the physical properties of these cationic derivatives, we speculate that the biological specificity of the active cationic derivatives either triggers endocytotic pathways leading to eventual endosomal fusion allowing cytoplasmic access to the packaged DNA or other endocytotic pathways that avoid lysosomal degradation.

**Keywords:** Cationic lipid; lipoplex; transfection; endosomal release; cell internalization; DC-Chol; TC-Chol

### Introduction

The use of cationic lipids as nonviral vectors to achieve therapeutic gene delivery is a well established concept owing to their decreased immunity effects, safety, and ease in production. Synthetic cholesterol-based cationic lipids are among the most promising agents and have been used with different levels of efficiency to safely deliver nucleic acid molecules to a variety of cells to achieve upregulation, gene replacement, and gene silencing.<sup>1,2</sup> One of the main characteristics of these systems is the inclusion of the helper lipid DOPE. Evidently, the presence of DOPE in

the formulation has been shown to improve transfection and lower cytotoxicity.<sup>1,3–5</sup> Certainly, the presence of DOPE not only encourages liposome formation and efficient plasmid DNA compaction, but it also plays a

\* To whom correspondence should be addressed. Mailing address: Long Island University, Pharmaceutical Sciences, 75 Dekalb Ave, Brooklyn, NY 11201. Tel: 718-488-1471. Fax: 718-780-4586. E-mail: msavva@liu.edu.

(1) Gao, X.; Huang, L. Cationic liposome-mediated gene transfer. *Gene Ther.* **1995**, *2*, 710–722.

- (2) Bajaj, A.; Kondiah, P.; Bhattacharya, S. Design, synthesis, and in vitro gene delivery efficacies of novel cholesterol-based gemini cationic lipids and their serum compatibility. *J. Med. Chem.* **2007**, *50* (10), 2432–2442.
- (3) Gao, X.; Huang, L. A novel cationic liposome reagent for efficient transfection of mammalian cells. *Biochem. Biophys. Res. Commun.* **1991**, *179* (1), 280–285.
- (4) Kiso, N.; Ariatti, M.; Moodley, T. A novel cationic cholesterol derivative, its formulation into liposomes, and the efficient transfection of the transformed human cell lines HepG2 and HeLa. *Drug Deliv.* **2002**, *9*, 161–167.
- (5) Congiu, A.; Pozzi, D.; Esposito, C.; Castellano, C.; Mossa, G. Correlation between structure and transfection efficiency: a study of DC-Chol - DOPE/DNA Complexes. *Colloids Surf. B. Biointerfaces.* **2004**, *36*, 43–48.

critical role in producing a structural conversion of the associated lipoplex leading to eventual destabilization of the endosomal membrane which affords DNA cytosolic access.<sup>6–9</sup>

Despite its beneficial effects in transfection efficiency, the universal use of DOPE in cholesterol-based lipoplex formulations has precluded meaningful structure–activity relationships for several reasons: First, studying the effect of systematic structural changes within these cationic lipid moieties on each step in relation to their transfection efficiency is very challenging simply because a three-component system, i.e., DNA, cationic lipid, and helper lipid, imposes on the system an enormous number of macroscopic phases.<sup>10</sup> Second, the presence of DOPE affects the physicochemical properties of lipoplexes and interferes with, modifies, or completely abolishes possible cationic lipid cell-specific interactions. A recent report published by Khalil and co-workers documented an increase in transfection possibly attributed to endosomal escape of low density octaarginine-modified liposomes in the presence of fusogenic lipids.<sup>11</sup> An increasing number of articles have emerged in the literature that investigate possible cholesterol-dependent endocytic pathways and intracellular trafficking of lipoplexes when formulated with DOPE.<sup>12–15</sup> In addition, studies with cationic cholesterol derivatives have demonstrated a correlation

between DNA condensation and transfection efficiency in the presence of DOPE.<sup>16</sup> In this study, we employ a simple two component mixture (cationic lipid and pDNA) to investigate the multidimensional relationship that is apparent between DNA binding, transfection, and endosomal release in the absence of DOPE.

Understanding the structure–activity relationship of the cationic hydrophilic region of cholesterol amphiphilic analogues will unequivocally give direction toward the development of safe and efficient gene delivery systems. Toward this end, four cholesterol-based cationic derivatives, that is, the well-known commercially available tertiary amine derivative  $3\beta$ -[N-(N',N'-dimethylaminoethane)carbamoyl]cholesterol hydrochloride (**5**, DC-Chol), the secondary amine derivative  $3\beta$ -[N-(N'-methylaminoethane)carbamoyl]cholesterol (**6**, MC-Chol), the primary amine analogue  $3\beta$ -[N-(aminoethane)carbamoyl]cholesterol (**7**, AC-Chol), and the quaternary ammonium salt  $3\beta$ -[N-(N',N',N'-trimethylaminoethane)carbamoyl]cholesterol iodide (**8**, TC-Chol), were synthesized in high purities. Cell internalization and transfection activity of lipoplexes without the inclusion of DOPE and in serum-free media were studied in two carcinoma cell lines. The results were correlated with the corresponding physicochemical properties of cationic lipids in isolation, their interaction with plasmid DNA and lipoplex formation, and their ability to fuse with negatively charged liposomes designed to mimic the endosomal compartment.

## Materials and Methods

**Materials.** Cholesteryl chloroformate 97%, iodomethane 99.5%, ethylenediamine 99%, N-methylethylenediamine 95%, N,N-dimethylethylenediamine 95%, 2-hydroxyethylmercaptan ( $\beta$ -mercaptoethanol), 3-(4,5-dimethylthiazol-2-yl)-2,5-diphenyltetrazolium bromide (MTT), o-nitrophenyl- $\beta$ -D-galactopyranoside (ONPG), and calcein were purchased from Sigma-Aldrich (St. Louis, MO). Tris(hydroxymethyl)aminomethane (ultrapure grade) and edetate disodium dihydrate (EDTA) were purchased from Spectrum Chemical Manufacturing Co. (New Brunswick, NJ). Sodium chloride, potassium chloride crystals, sodium phosphate monobasic and dibasic, potassium phosphate monobasic, magnesium chloride, and Triton X-100 were purchased from Fisher Scientific (Suwanee, GA). Epidermal mouse melanoma cells (B16F0), human cervical carcinoma cells (HeLa), and Dulbecco's modified Eagle's medium (DMEM) were obtained from American Type Culture Collection (Manassas, VA). Fetal calf serum, penicillin (5000 units)/streptomycin (5000  $\mu$ g), and ethidium bromide solution (10 mg/mL) were obtained from Invitrogen Corp. (Grand Island, NY). 1,2-Dioleoyl-3-trimethylammonium-propane (DOTAP), 1,2-dioleoyl-*sn*-glycero-3-phosphocholine (DOPC), 1,2-dioleoyl-*sn*-glycero-3-phosphoethanolamine (DOPE), and 1,2-diacyl-*sn*-glycero-3-[phospho-*rac*-(1-glycerol)] (DOPG) were purchased from Avanti Polar Lipids, Inc. (Alabaster, AL). The fluorescein labeling reagent together with the G50 microspin columns (Label IT Fluorescein Labeling Kit) was purchased from Mirus Bio Corp. (Madison, WI). Solvents from commercial suppliers were of reagent grade and were used

- (6) Farhood, H.; Serbina, N.; Huang, L. The role of dioleoyl phosphatidylethanolamine in cationic liposome mediated gene transfer. *Biochim. Biophys. Acta* **1995**, 1235 (2), 289–295.
- (7) Chesnoy, S.; Huang, L. Structure and function of lipid-DNA complexes for gene delivery. *Annu. Rev. Biophys. Biomol. Struct.* **2000**, 29, 27–47.
- (8) Koyanova, R.; Wang, L.; Tarahovsky, Y.; MacDonald, R. C. Lipid phase control of DNA Delivery. *Bioconjugate Chem.* **2005**, 16 (6), 1335–1339.
- (9) Wasungu, L.; Hoekstra, D. Cationic lipids, lipoplexes and intracellular delivery of genes. *J. Controlled Release* **2006**, 116 (2), 255–264.
- (10) May, S.; Harries, D.; Ben-Shaul, A. The phase behavior of cationic lipid-DNA complexes. *Biophys. J.* **2000**, 78, 1681–1697.
- (11) Khalil, I.; Kogure, K.; Futaki, S.; Harashima, H. High density of octaarginine stimulates macropinocytosis leading to efficient intracellular trafficking for gene expression. *J. Biol. Chem.* **2006**, 281 (6), 3544–3551.
- (12) Zuhorn, I.; Kalicharan, R.; Hoekstra, D. Lipoplex-mediated transfection of mammalian cells occurs through the cholesterol-dependent clathrin-mediated pathway of endocytosis. *J. Biol. Chem.* **2002**, 277 (20), 18021–18028.
- (13) Prasad, T.; Rangaraj, N.; Rao, N. Quantitative aspects of endocytic activity in lipid-mediated transfections. *FEBS Lett.* **2005**, 579 (12), 2635–2642.
- (14) Payne, C.; Jones, S.; Chen, C.; Zhuang, X. Internalization and trafficking of cell surface proteoglycans and proteoglycan-binding ligands. *Traffic* **2007**, 8 (4), 389–401.
- (15) Hoekstra, D.; Reijman, J.; Wasung, F.; Zuhorn, I. Gene delivery by cationic lipids: in and out of an endosome. *Biochem. Soc. Trans.* **2007**, 35 (Pt 1), 68–71.
- (16) Geall, A.; Eaton, M.; Baker, T.; Catterall, C.; Blagborough, I. The regiochemical distribution of positive charges along cholesterol polyamine carbamates plays significant roles in modulating DNA binding affinity and lipofection. *FEBS Lett.* **1999**, 459, 337–342.

without further purification. NMR spectra were recorded on a Varian 400 MHz Inova spectrometer with a deuterated solvent as the internal lock.

**Synthesis. 3 $\beta$ -[N-(N',N'-Dimethylaminoethane)carbamoyl]cholesterol (5, DC-Chol).** N,N-Dimethylethylenediamine **1** (2.5 mL, 22.5 mmol) was dissolved in 25 mL of anhydrous chloroform in an oven-dried reaction flask. Cholesteryl chloroformate **4** (2.0 g, 4.5 mmol) was dissolved in a minimum amount of anhydrous chloroform and added dropwise to the reaction flask on an ice bath. The reaction mixture was stirred at room temperature for approximately 30 min, extracted several times with chloroform, and washed with saturated brine and saturated sodium carbonate. The organic layer was combined, dried with sodium sulfate, and concentrated under reduced pressure using rotary evaporator. The product was eluted with CHCl<sub>3</sub>/CH<sub>3</sub>OH (9:1 v/v) from a silica gel (70–230 mesh, 60 Å), and the solvent was removed under reduced pressure to give **5** as a light yellowish solid (2.0 g, 80%) yield, *R*<sub>f</sub> = 0.57 (CHCl<sub>3</sub>/CH<sub>3</sub>OH 4:1 v/v). The presence of the cholesterol backbone was confirmed with cholesterol stain which gave a purple spot on TLC.<sup>17</sup> Gaseous hydrogen chloride was flushed into a chloroform solution of **5** to yield the DC-Chol hydrochloride salt as a white powder (99%). Anal. Calcd for C<sub>32</sub>H<sub>56</sub>N<sub>2</sub>O<sub>2</sub> (MW 501): C, 76.75; H, 11.27; N, 5.59. Found: C, 76.60; H, 11.52; N, 5.45. MS (positive/negative ES): *m/z* 501.5 [M + H]<sup>+</sup>. <sup>1</sup>H NMR (400 MHz, CDCl<sub>3</sub>, 20 °C, TMS): δ 0.63 (s, 3H, CH<sub>3</sub> 18), 0.82–0.84 (d, 6H, CH<sub>3</sub> 26–27), 0.87–0.90 (d, 3H, CH<sub>3</sub> 21), 0.97 (s, 3H, CH<sub>3</sub> 19), 2.70 (m, 2H, NHCH<sub>2</sub>), 2.95 (s, 6H, N(CH<sub>3</sub>)<sub>2</sub>), 3.35 (m, 2H, OCONHCH<sub>2</sub>), 4.45 (m, 1H, H'3), 5.35 (d, 1H, *J* = 5, H'6).

The same synthetic method was used for compounds **6** and **7** as shown in Scheme 1.

**3 $\beta$ -[N-(N'-Methylaminoethane)carbamoyl]cholesterol (6, MC-Chol).** Anal. Calcd for C<sub>31</sub>H<sub>54</sub>N<sub>2</sub>O<sub>2</sub> (MW 487): C, 76.43; H, 11.51; N, 5.75. Found: C, 76.07; H, 11.69; N, 5.62. MS (positive/negative ES): *m/z* 487.7 [M + H]<sup>+</sup>. <sup>1</sup>H NMR (400 MHz, CDCl<sub>3</sub>, 20 °C, TMS): δ 0.63 (s, 3H, CH<sub>3</sub> 18), 0.82–0.85 (d, 6H, CH<sub>3</sub> 26–27), 0.87–0.89 (d, 3H, CH<sub>3</sub> 21), 0.97 (s, 3H, CH<sub>3</sub> 19), 2.80 (t, 2H, NHCH<sub>2</sub>), 2.90 (d, 3H, NHCH<sub>3</sub>), 3.35 (m, 2H, OCONHCH<sub>2</sub>), 4.45 (m, 1H, H'3), 5.35 (d, 1H, *J* = 5, H'6).

**3 $\beta$ -[N-(Aminoethane)carbamoyl]cholesterol (7, AC-Chol).** Anal. Calcd for C<sub>30</sub>H<sub>52</sub>N<sub>2</sub>O<sub>2</sub> (MW 473): C, 76.11; H, 10.99; N, 5.93. Found: C, 75.94; H, 11.25; N, 5.93. MS (positive/negative ES): *m/z* 472.7 [M + H]<sup>+</sup>. <sup>1</sup>H NMR (400 MHz, CDCl<sub>3</sub>, 20 °C, TMS): δ 0.63 (s, 3H, CH<sub>3</sub> 18), 0.82–0.85 (d, 6H, CH<sub>3</sub> 26–27), 0.87–0.89 (d, 3H, CH<sub>3</sub> 21), 0.97 (s, 3H, CH<sub>3</sub> 19), 2.80 (t, 2H, NHCH<sub>2</sub>), 3.20 (m, 2H, OCONHCH<sub>2</sub>), 4.45 (m, 1H, H'3), 4.90 (m, 1H, OCONH), 5.35 (d, 1H, *J* = 5, H'6).

**3 $\beta$ -[N-(N',N',N'-Trimethylaminoethane)carbamoyl]cholesterol Iodide (8, TC-Chol).** To a solution of **5** (0.50 g, 1 mmol) in 15 mL of absolute ethanol was added dropwise methyl iodide (56 μL, 1.2 mmol) at room temperature, as shown in Scheme 1. The reaction mixture was refluxed for 2 h and purified by silica gel chromatography (5% MeOH/

CHCl<sub>3</sub>) to yield 400 mg (75%) of a light yellowish solid. *R*<sub>f</sub> = 0.35 (CHCl<sub>3</sub>/CH<sub>3</sub>OH 4:1 v/v). Anal. Calcd for C<sub>33</sub>H<sub>60</sub>N<sub>2</sub>O<sub>2</sub> (MW 643): C, 61.47; H, 9.54; N, 4.3. Found: C, 59.97; H, 9.36; N, 4.10. MS (positive/negative ES): *m/z* 515.4 [M + H]<sup>+</sup>, 516.4 [cation of salt]. <sup>1</sup>H NMR (400 MHz, CDCl<sub>3</sub>, 20 °C, TMS): δ 0.63 (s, 3H, CH<sub>3</sub> 18), 0.82–0.85 (d, 6H, CH<sub>3</sub> 26–27), 0.87–0.89 (d, 3H, CH<sub>3</sub> 21), 0.97 (s, 3H, CH<sub>3</sub> 19), 3.44 (s, 9H, N(CH<sub>3</sub>)<sub>3</sub>), 3.75–3.86 (m, 4H, NCH<sub>2</sub>CH<sub>2</sub>N), 4.45 (m, 1H, H'3), 5.35 (d, 1H, *J* = 5, H'6), 6.15 (s, 1H, OCONH).

**Plasmid DNA.** Both plasmid DNA vectors were amplified in DH5α competent cells, purified, and quantified as described elsewhere.<sup>18</sup>

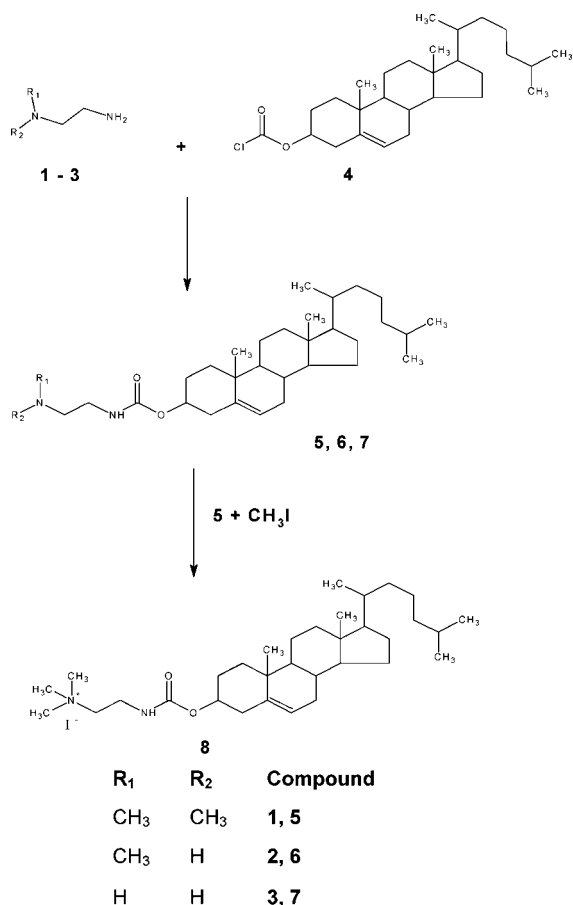
**Preparation of Liposomal Dispersions.** Cationic carbamoyl cholesterol lipid derivatives (0.6 mmol) were transferred from chloroform solutions into borosilicate glass tubes. The solvents were evaporated using a dry nitrogen stream to produce thin lipid films on the bottom of the tubes. Any residual solvent was removed via a vacuum pump overnight. Anhydrous lipid films were hydrated by the addition of 1 mL of 40 mM Tris to allow for self-assembly of cholesterol molecules followed by agitation via vortexing and sonication in a bath sonicator to disrupt any large aggregates in the dispersions. A temperature of 60 °C was maintained for the duration of the hydration period (1 h). The stability of DC-Chol in isolation was verified after heating the lipid dispersion at 60 °C for 1 h followed by comparison with DC-Chol from the stock solution using TLC. Prior to the use of all derivatives in each experiment, suspensions were vortexed and sonicated for approximately 2 min.

**Lipofection.** Two cell lines, B16F0 and HeLa, were transfected with dispersions of each carbamoyl cholesterol derivative complexed with plasmids encoding β-galactosidase and green fluorescent protein to obtain quantitative and qualitative information, respectively. The expression of both plasmids is under the control of the human cytomegalovirus (CMV) immediate early promoter.

Both cell lines were cultured at 37 °C in a 5% CO<sub>2</sub> humidified atmosphere in DMEM supplemented with 10% fetal calf serum (complete medium), 100000 U/L penicillin, and 50 mg/L streptomycin. Twelve hours before transfection, approximately 50000 cells were seeded into the wells of a 48-well plate and incubated to achieve a monolayer with 50–70% confluence. Lipoplexes were prepared in serum-free media 20–30 min prior to transfection by incubating aliquots of each lipid dispersion with plasmid DNA at +/– charge ratios of 1:1, 2:1, 4:1, 7:1, and 10:1. The pDNA concentration was held constant at 1.0 μg/well. As a negative control, pDNA without lipid was added to the cells and assayed for β-galactosidase activity. As a positive control, cells were

(17) Kates, M. *Techniques of Lipidology: Isolation, Analysis and Identification of Lipids*; American Elsevier; New York, 1975; pp 437–440.

(18) Sheikh, M.; Feig, J.; Gee, B.; Li, S.; Savva, M. In vitro lipofection with novel series of symmetric 1,3-dialkoylamidopropane-based cationic surfactants containing single primary and tertiary amine polar head groups. *Chem. Phys. Lipids* **2003**, *124* (1), 49–61.

**Scheme 1.** Synthetic Scheme for the Preparation of Cholesterol-Based Cationic Lipids

lipofected with DOTAP/pDNA at a ratio of 2:1. Treated cells were incubated at 37 °C with 5% CO<sub>2</sub> for 4 h, during which time lipofection was allowed to occur. After the duration of the transfection, the serum-free media (SFM) used during the transfection was removed and the cells were supplemented with 500  $\mu$ L of fresh complete medium.

Approximately 48 h post-transfection, complete media was removed via gentle aspiration from monolayers of transfected cells cultured in 48-well plates. The cells were washed twice with cold phosphate-buffered saline pH 7.4 (137 mM NaCl, 2.7 mM KCl, 10 mM Na<sub>2</sub>HPO<sub>4</sub>, 2 mM KH<sub>2</sub>PO<sub>4</sub>) to remove any residual media. Plates were kept on ice for the duration of the assay. Cell lysis was accomplished by incubating the cells for 15 min in a detergent-containing lysis buffer pH 7.2 (0.1 M Tris, 0.1% w/v Triton X). Cell disruption was achieved by repetitive pipeting, followed by collection of the cell lysates in microfuge tubes. The resulting cell suspensions were centrifuged at 14,000 rpm for 10 min at 4 °C, after which time the supernatant was recovered for the subsequent assay in a 96-well microtiter plate. A volume of 5–50  $\mu$ L of cell lysate was used per reaction. Lysis buffer without any cell lysate and cell lysates of untreated cells were used as a negative control. An equal volume of assay buffer pH 7.3 (100 mM NaH<sub>2</sub>PO<sub>4</sub>, 100 mM Na<sub>2</sub>HPO<sub>4</sub>, 2 mM MgCl<sub>2</sub>, 100 mM  $\beta$ -mercaptoethanol) containing the substrate ONPG at a concentration of 1.33 mg/mL was added to the

wells and incubated for approximately 30 min to allow any  $\beta$ -galactosidase present to hydrolyze the colorless substrate to the yellow colored *o*-nitrophenol derivative. Termination of the reaction was achieved by the addition of a 1 M sodium carbonate solution. The absorbance of each sample was read in a plate reader at 405 nm and was compared with standard curves prepared with concentrations of  $\beta$ -galactosidase between 0.005 and 10 mU/ $\mu$ L.

#### Fluorescence Microscopy of Transfected B16F0 Cells.

To prevent rapid quenching of the fluorescence during analysis, the plasmid DNA used was the pEGFP-C3 which encodes a red-shifted variant of the wild-type green fluorescent protein (GFP) reporter gene which has been optimized for brighter fluorescence (excitation maximum = 488 nm; emission maximum = 507 nm) and higher expression in mammalian cells.<sup>19</sup>

For qualitative analysis, photographs were taken approximately 48 h post-transfection using the Zeiss fluorescent inverted microscope (Axiovert 200M) equipped with a FITC fluorescence filter.

To determine the location of lipoplexes B16F0, cell lines were transfected with fluorescently labeled DNA. Plasmid DNA was covalently and nondestructively labeled with fluorescein-labeling reagent at a label to nucleotide ratio of 40–120 according to the accompanying protocol. Purification of the labeled nucleic acid samples was performed using G50 microspin columns. Cell transfections were performed as described above by modifying the ratios of labeled to unlabeled plasmid until optimal fluorescence intensity was achieved (15%). After a 4 h treatment time, the serum-free media containing the lipoplex preparation was aspirated from the wells and the cells were washed twice with PBS warmed to 37 °C to remove excess noncellular associated fluorescent lipoplexes. Images of the transfected cells were obtained in a manner similar to that of the GFP images.

**Cytotoxicity.** Approximately 42 h post-transcription, 50  $\mu$ L of 5 mg/mL of 3-(4,5-dimethylthiazol-2-yl)-2,5-diphenyltetrazolium bromide (MTT) was added to the wells of both cell lines and further incubated for 4 h at 37 °C. Mitochondrial dehydrogenase enzymes of viable cells have the ability to cleave the tetrazolium rings of the MTT to form dark blue formazan crystals during that time period. Subsequent addition of 250  $\mu$ L of DMSO to the cells resulted in membrane disruption and solubilization of the crystals. The resulting color was quantified by measuring the absorbance using a multiwell plate reader at 630 nm on the basis that the amount of formazan crystals detected is directly proportional to the number of viable cells. Untreated cells were used as a negative control. Values were normalized against the value of the negative control which was assigned a value of 100%.

**Agarose Gel Electrophoresis.** The complexation ability of the carbamoyl cholesterol cationic derivatives with plas-

(19) Cormack, B. P.; Valdivia, R. H.; Falkow, S. FACS-optimized mutants of the green fluorescent protein (GFP). *Gene* **1996**, *173* (1), 33–38.

mid DNA was analyzed by agarose gel electrophoresis. Electrophoretic equipment utilized in this assay was obtained from BioRad. The gel mold provided with the apparatus was filled to an approximate thickness of 5.0 mm with standard agarose in a 16 mM TAE buffer pH 7.2 (40 mM Tris acetate, 1.14 mL of glacial acetic acid, 1.0 mM EDTA) solution. The concentration of the gel used in this retardation assay was 0.8%; a percentage selected to resolve any migration of DNA molecules in the range of 7 kb. Ethidium bromide was added to the gel-solution at a concentration of 0.5  $\mu\text{g/mL}$  for visualization of any migrated DNA. DNA migration was facilitated using an applied voltage of 5V per centimeter of casted gel for 30–45 min.

Lipoplexes were formulated at  $\pm$  charge ratios of 0.5:1, 1:1, 2:1, 4:1, 6:1, and 8:1. Samples were prepared in microcentrifuge tubes by the addition of 0.2  $\mu\text{g}$  of DNA followed by cationic lipid to achieve each desired charge ratio. Appropriate volumes of 40 mM Tris buffer and serum-free media (SFM) were added to achieve a final volume of 10  $\mu\text{L}$ . Lipoplex samples were centrifuged at room temperature for 10 s at a speed of 14000 rpm, and then allowed to stand at room temperature for 30 min. Prior to loading each sample into the wells of each gel, 1  $\mu\text{L}$  of a 0.25% bromophenol solution (30.0% glycerol, 0.25% bromophenol blue, 0.25% xylene cyanol FF) was added to each sample. As a negative control, naked DNA was added to each gel in the first and last lanes. After a 30–45 min migration period, the gel was viewed with a UV light source and photographed with a Gel logic 200 imaging system connected to a Kodak 1D Scientific Imaging System (Eastman Kodak Company, New Haven, CT).

**Ethidium Bromide Displacement.** Ethidium bromide (EtBr) displacement from plasmid DNA was utilized in this study as a measurement of the lipids' ability to condense plasmid DNA. Experiments were carried out in 40 mM Tris buffer as well as in SFM and were conducted on a Cary Eclipse Fluorescence spectrophotometer (Varian, Inc.) at excitation and emission wavelengths of 515 and 605 nm, respectively, as described elsewhere.<sup>20</sup>

**Photon Correlation Spectroscopy (PCS) and Electrophoretic Mobility ( $\zeta$  Potential).** Particle size and  $\zeta$  potential of lipid dispersions were analyzed using the Malvern Zetasizer Nano system (Malvern Instruments, Inc., Southborough, MA) in 40 mM Tris buffer and SFM which uses HEPES buffer as a base. Lipid dispersions ( $\sim 120$  nmol) were added to cuvettes followed by the addition of 40 mM Tris buffer pH 7.2 or SFM as necessary, to a final volume of 1.2 mL. Plasmid DNA was subsequently added in ratios equivalent to those used in the transfection experiments. The resulting mixtures were incubated while stirring for 10 min, after which time the scattered light intensity of each sample at a 90° angle was measured at 23 °C. The reported

hydrodynamic diameter distributions were derived using the Zetasizer Nano system's self-analyzing autocorrelation function. The polydispersity indices corresponding to the widths of each size distribution correlation curve was a parameter derived from the cumulants analysis method embedded within the software.

The  $\zeta$  potential of the aqueous vesicles was determined with and without the incorporation of plasmid DNA in 40 mM Tris buffer pH 7.2. After measuring the particle distribution within each sample, 0.75 mL (0.1  $\mu\text{mol}$ ) was withdrawn using a 1 mL tuberculin syringe and placed in the Zetasizer's folded capillary cell for  $\zeta$ -potential measurement.

**Interfacial Studies.** Stock solutions of cationic lipids were prepared in chloroform from which aliquots were used for monolayer deposition at an air/water interface for subsequent analysis.  $\Pi$ -A analysis of monolayer films were carried out with the aid of a PC controlled analytical film balance (KSV Instruments Ltd., Helsinki, Finland). The configuration of the apparatus enabled symmetric compression of monolayers spread at an air/water interface. Isothermal compression of each monolayer was achieved by maintaining the subphase (150 mL of 40 mM Tris buffer, pH 7.2) at desired temperature with the aid of an external water circulator attached to coils incorporated in the base of the trough. Phase transitions and monolayer collapse of each compression isotherm were determined as described elsewhere.<sup>21</sup> To further characterize the interaction forces within lipid monolayers, the compressibility modulus,  $K$  was obtained at monolayer collapse, using a two-dimensional form of the bulk modulus, that is calculated using the following equation:

$$K = -A \left( \frac{\partial \Pi}{\partial A} \right)_T$$

**Fusion Assay.** Lipid films composed of 20 mM DOPC/DOPE/DOPG 1:2:1 were prepared as described above for the cationic lipid (CL) films. Calcein was encapsulated in vesicles prepared by hydrating the lipid films with a 50 mM calcein solution. Unencapsulated material was separated from vesicles using a Sephadex G-25 column with HBS pH 7.0, as the elution buffer which allowed for the proper interpretation of and correlation with the physical data obtained from experiments performed with the HEPES based serum free media. Calcein leakage from the negatively charged liposomes was induced at 37 °C by adding concentrations of each cholesterol derivative equal to those which mediated efficient cell transfection, while keeping the PC/PE/PG concentration constant. Those concentrations were equivalent to molar lipid ratios CL:(PC/PE/PG) of 56:1, 113:1 and 225:1. The fluorescence signal resulting from the dequenching of calcein upon release into the suspending medium was obtained with a Cary Eclipse fluorescence spectrophotometer

(20) Savva, M.; Chen, P.; Aljaberi, A.; Selvi, B.; Spelios, M. In vitro lipofection with novel asymmetric series of 1,2-dialkoylamidopropane-based cytofectins containing single symmetric bis-(2-dimethylaminoethane) polar headgroups. *Bioconjugate Chem.* **2005**, 16 (6), 1411–1422.

(21) Aljaberi, A.; Chen, P.; Savva, M. Synthesis, in vitro transfection activity and physicochemical characterization of novel N,N'-diacyl-1,2-diaminopropyl-3-carbamoyl-(dimethylaminoethane) amphiphilic derivatives. *Chem. Phys. Lipids* **2005**, 133 (2), 135–149.

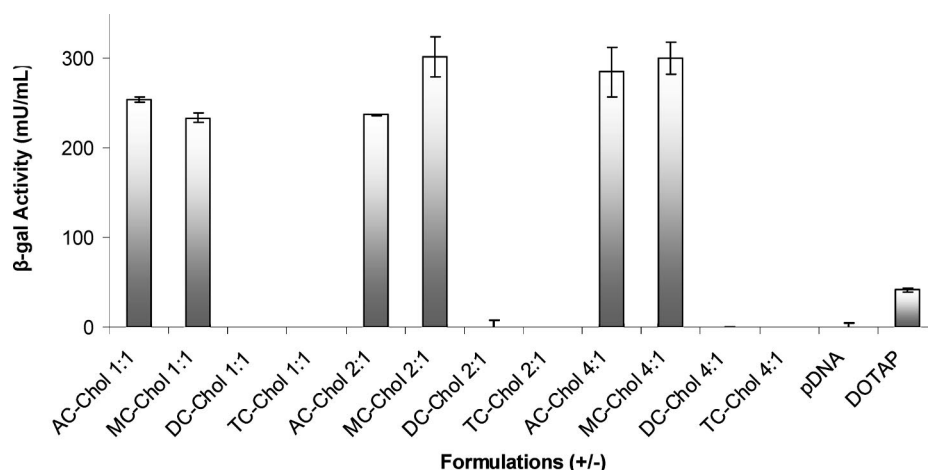


**Figure 1.** Lipofection of AC-Chol, MC-Chol, DC-Chol, and TC-Chol at CL/DNA ratios of 1:1, 2:1, and 4:1 in mouse melanoma cells (B16F0). The data presented is representative of the average  $\beta$ -galactosidase concentrations performed in triplicate for six different transfections.

using the following specifications:  $\lambda_{\text{ex}} = 490 \text{ nm}$ ,  $\lambda_{\text{em}} = 520 \text{ nm}$ , ex slit = 5 nm, em slit = 2.5 nm. The fluorescence intensity of integral vesicles was used as 0% leakage ( $F_0$ ). Maximum fluorescence ( $F_{\text{max}}$ ) was determined by lysing vesicles with triton-X. The percent of calcein leakage was determined using the following equation:

$$\frac{F - F_0}{F_{\text{max}} - F_0} \times 100$$

## Results and Discussion

While it is accepted that cationic lipids begin the process of lipofection by binding to the negatively charged cell surface proteoglycans, the influence of their chemistry on eliciting an endocytic response due to specific cationic lipid-cell surface interactions has not been examined. This is especially true with respect to polar methylation on cholesterol-based analogues, and accordingly, this study scrutinizes the chemistry of four amphiphilic headgroup domains while maintaining a constant hydrophobic cholesterol domain. Our preference for cholesterol derivatives instead of double-chained cationic lipids lies in the lack of pH- and temperature-dependent phase transitions in their aggregate structures. To this end, our studies on transfection activities of these cholesterol-based cationic derivatives were performed in the absence of serum and without the inclusion of DOPE in the formulations. No such studies were ever reported in the literature for the two novel derivatives, AC-Chol and MC-Chol, nor for the commercially available DC-Chol and TC-Chol. We began by comparing the level of efficiency at which these derivatives mediated lipofection in two different cell lines (mouse melanoma and human carcinoma). Both quantitative ( $\beta$ -galactosidase) and qualitative (EGFP and FITC labeled pDNA) transfection data performed in those cell lines are presented below which clearly differentiate the efficiency of two newly synthesized primary (AC-Chol) and secondary (MC-Chol) cholesterol analogues to mediate transfection in the absence of a helper lipid. We subsequently

determined the localization of lipoplexes post-transfection and correlated their structural specificity with their activity, physicochemical characteristics, interfacial properties, and their ability to rupture negatively charged synthetic liposomes that resemble the composition of endosomal membranes.

**In Vitro Lipofection and Cytotoxicity.** Aqueous dispersions of a series of carbamoyl cholesterol cationic lipids in the absence of helper lipids were examined for their ability to transfect B16F0 and HeLa cells. All cell transfections and physicochemical analysis were carried out with DC-Chol hydrochloride as opposed to the free base given the inability of the latter to hydrate and form stable dispersions in aqueous media. Of the four derivatives investigated, the most effective mediators of cell transfection were AC-Chol and MC-Chol, which elicited higher  $\beta$ -galactosidase activities when compared with their tertiary and quaternary counterparts. Concentrations representing activity were indiscernible at charge ratios of 1:1, 2:1 and 4:1 in the B16F0 cell line (Figure 1), with a range between 230 – 300 mU/mL. Significantly lower levels of  $\beta$ -galactosidase activity were observed at charge ratios 1:1 and 2:1 in the HeLa cell line while no activity was observed at charge ratio 4:1 (Figure 2). Higher CL:DNA ratios of 7:1 and 10:1 failed to induce  $\beta$ -galactosidase activity in either cell line due to toxicity (results not shown).

The efficiency of lipofection was also confirmed with the expression of the genetically engineered green fluorescence protein in B16F0 cells (Figure 3). In keeping with the results obtained by the  $\beta$ -galactosidase assay, the most effective mediation of cell transfection was observed at ratios 1:1, 2:1, and 4:1 with AC-Chol and MC-Chol. Representative images of transfection at ratio 2:1 are shown for AC-Chol and MC-Chol (Figure 3a and b, respectively). Expression of green fluorescent protein was not detected in transfections using DC-Chol and TC-Chol (Figure 3c and d, respectively).

No significant difference in the cytotoxicity of cationic lipids was observed in each cell line at the active charge ratios, whereas application of the inactive formulations to both cell lines resulted in a significant decrease in cell

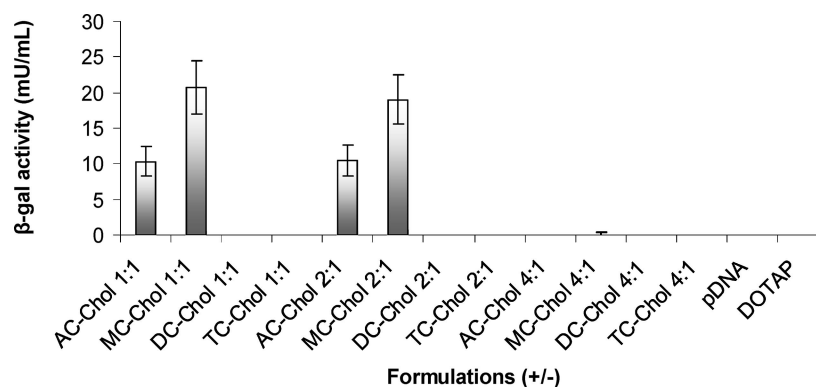


**Figure 2.** Lipofection of AC-Chol, MC-Chol, DC-Chol, and TC-Chol at CL/DNA ratios of 1:1, 2:1, and 4:1 in human cervical carcinoma cells (HeLa). The data presented is representative of the average  $\beta$ -galactosidase concentrations performed in triplicate for six different transfections.

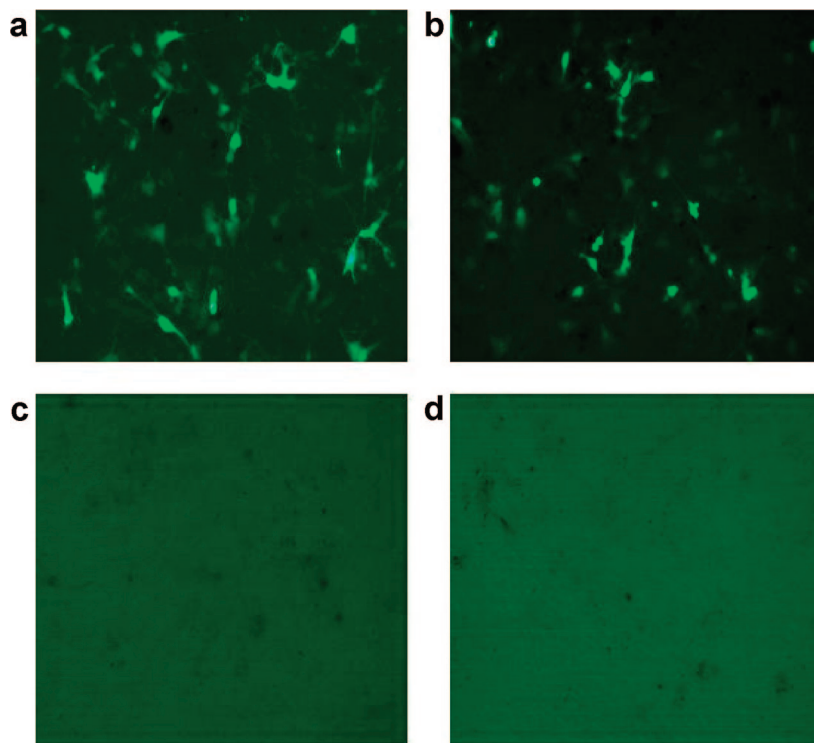


**Figure 3.** Lipofection efficiency in B16F0 cells mediated by each of the four carbamoyl cholesterol derivatives complexed with the EGFP plasmid. Since transfection activity at charge ratios (+/-) 1:1, 2:1, and 4:1 was not significantly different for each pair of active (AC-Chol and MC-Chol) and nonactive (DC-Chol and TC-Chol) derivatives, one representative image (+/- 2:1) was chosen per lipid. Images a, b, c, and d represent AC-Chol, MC-Chol, DC-Chol, and TC-Chol, respectively.

viability (Figure 4). The lowest percentage of viable cells was observed in the HeLa cell line at charge ratio 4:1 with 15% viability after the application of TC-Chol to the cells and 41% viability after applying DC-Chol to the cells.

**Cell Internalization Studies.** The higher  $\beta$ -galactosidase concentrations and the expression of the green fluorescent protein confirmed efficient delivery of fluorescently labeled DNA to the cell's interior using the novel AC-Chol and MC-Chol analogues. To further investigate possible reasons for the inability of the other two derivatives to mediate cell transfection, lipoplexes were formed with fluorescein-labeled plasmid DNA. The images presented in Figure 5 were taken after the cells were washed with PBS to allow a 2-fold visual inspection regarding the

location of the lipoplexes. Cell internalized and lipoplexes that are associated with the cell membrane are clearly depicted using the active lipid formulations AC-Chol and MC-Chol (Figure 5a and b, respectively), while diffused fluorescence at significantly lower amounts and at much lower levels of intensity (lack of bright spots) is observed only at the surface of the cells transfected with DC-Chol and TC-Chol (Figure 5c and d, respectively). These transfection experiments performed with FITC-labeled pDNA complement the other lipofection studies and the calcein leakage experiments (see Fusion Assay) and provide definitive results; i.e., there is little to no  $\beta$ -galactosidase concentrations measured, no fluorescence observed with the EGFP plasmid, and little to no

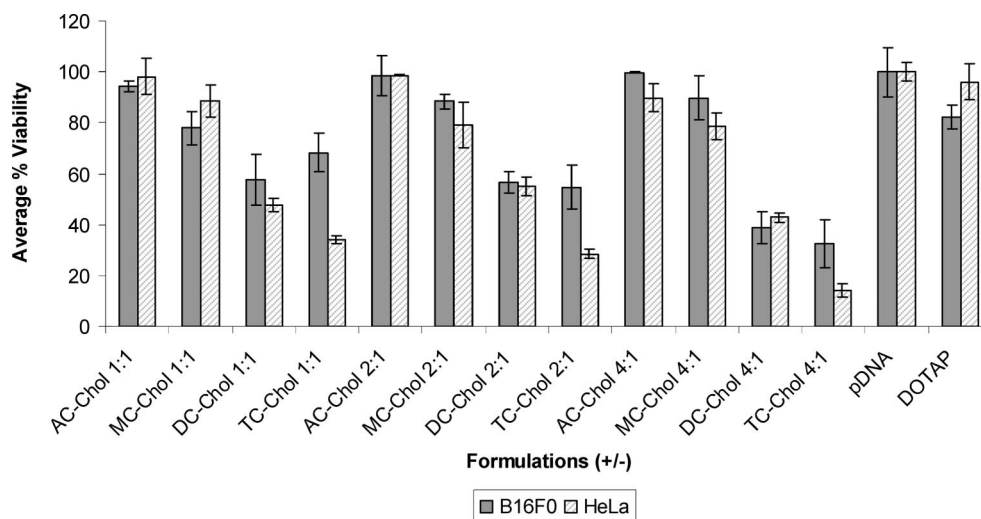


**Figure 4.** Cytotoxicity of AC-Chol, MC-Chol, DC-Chol, and TC-Chol at the most active CL/DNA ratios of 1:1, 2:1, and 4:1 in B16F0 cells (solid bars) compared with HeLa cells (stripped bars). The data presented is representative of the average of three separate experiments, each one performed in triplicate.

fluorescence observed with the FITC labeled DNA using DC-Chol and TC-Chol.

**DNA Complexation and Compaction Studies.** Complexation and compaction of plasmid DNA was studied in 40 mM Tris buffer and serum-free media to compare the effects of the high ionic strength environment on the formulations, since the lipoplexes were diluted in the latter environment prior to carrying out the cell transfections. Complexation was analyzed based on their ability to inhibit DNA migration through an agarose gel matrix. In 40 mM Tris buffer, AC-Chol, MC-Chol, and DC-Chol were able to complex fully with and retard pDNA migration at charge ratio  $\geq 4:1$ , while partial complexation was observed at CL/DNA  $\leq 2:1$  (Figure 6a). TC-Chol was able to fully complex with DNA at a charge ratio of 2:1. Complexation was less efficient in serum free media overall. AC-Chol, MC-Chol, and DC-Chol fully complexed with plasmid DNA at charge ratio  $\geq 6:1$  (Figure 6b), while TC-Chol fully retarded migration at a charge ratio  $\geq 4:1$  with partial complexation at ratio  $\leq 2:1$  (Figure 6b, lanes 5 and 4, respectively).

A plot of the normalized displacement in Tris buffer (Figure 7a) indicates that active lipids AC-Chol and MC-Chol are able to condense approximately 45% of the initial concentration of DNA at a charge ratio of 2:1. Parabolic curve fitting of the ethidium bromide dissociation curves for AC-Chol and MC-Chol in Tris buffer (Figure 7a) agrees with the gel electrophoresis data and reveals complete condensation at a ratio of approximately 3:1, indicating their ability to compact the plasmid DNA to which they complexed offering necessary protection. In comparison, DC-Chol and TC-Chol ineffectively interact with DNA at charge ratio 2:1 and are only able to displace 20% of the intercalated EtBr. Thus, binding of DC-Chol and TC-Chol to plasmid DNA as supported by gel electrophoresis experiments (Figure 6a) failed to induce plasmid DNA condensation in Tris buffer (Figure 7a). Ethidium bromide displacement from DNA in SFM mediated by AC-Chol and MC-Chol was 35 and 50%,

respectively (Figure 7b). The inactive lipid DC-Chol mediated a 30% while the quaternary ammonium derivative TC-Chol mediated a significantly higher 65% displacement of EtBr. Apparently at high ionic strength the ability of TC-Chol for DNA compaction increased significantly (Figure 7b), although the gel electrophoresis experiments have indicated that the complexation of TC-Chol with plasmid DNA was adversely affected at high ionic strength. It is important to emphasize that these two results do not contradict each other. Complete neutralization of the negative charge of the DNA is accomplished at  $\pm$  charge ratios  $> 2$  (Figure 7b). Reduced hydration of the cationic lipid and dehydration of plasmid DNA is promoted at high salt concentrations and both facilitate tighter packing of TC-Chol and more efficient DNA compaction. However, attenuation of electrostatic forces due to the pronounced “screening effect” in high ionic strength media slightly increased the TC-Chol concentration required to fully neutralize the negative charge of the plasmid DNA.<sup>20</sup>

These results indicate that binding of the cholesterol-based cationic lipids yielding weak to moderate condensation of plasmid DNA to particles of size around 1  $\mu\text{m}$  (see next section), in the absence of serum, is a characteristic property of active lipoplexes.

**Particle Size and  $\zeta$  Potential Studies.** Association between the cationic lipids and the plasmid DNA was also confirmed by measurements of lipoplex particle size together with the electrophoretic mobility of the lipid dispersions with and without the inclusion of DNA (Table 1). The size distributions of lipid dispersions formed in 40 mM Tris buffer without the inclusion of DNA had a hydrodynamic diameter range of 140–200 nm. Upon addition of DNA, the particle size increased slightly at 1:1 and 2:1 charge ratio, while significantly larger assemblies were observed at charge ratio 4:1. The polydispersity indices of all samples except DC-Chol and TC-Chol at charge ratio 4:1 were  $\leq 0.3$ , suggesting fairly monodisperse colloidal dispersions. Lipoplexes of DC-

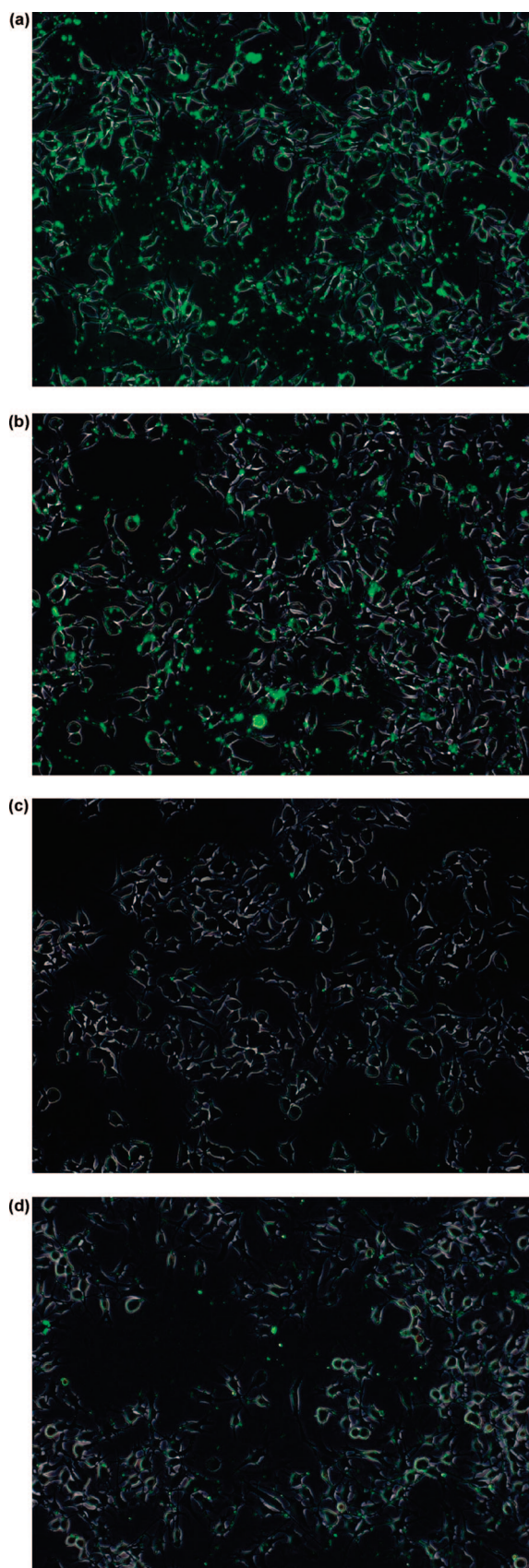


**Figure 5.** B16F0 cells transfected with fluorescently labeled plasmid DNA. Depicted are representative images of AC-Chol (a), MC-Chol (b), DC-Chol (c), and TC-Chol (d) at  $\pm 2:1$ .

Chol and TC-Chol produced PDI values of 0.80 and 0.99, respectively, indicating polydisperse samples.

Particle size distributions obtained in physiological ionic strength conditions compared with 40 mM Tris buffer differed significantly for AC-Chol and MC-Chol dispersions in isolation. Also, at charge ratios 1:1 and 2:1, the two active lipids showed significant differences in lipoplex size in the two dispersants. Interestingly, dispersions containing DC-Chol did not reveal significant differences in particle size distributions under high ionic strength conditions, whereas the size distribution of TC-Chol increased with respect to charge ratio resulting in the formation of very large particles at 4:1.

The  $\zeta$  potential measurements confirmed the association between the cationic lipids and DNA under low ionic strength conditions, since the  $\zeta$  potential became positive as the concentration of lipid increased. Contrary to the experiments carried out in 40 mM Tris, lipid dispersions in SFM exhibited significantly reduced  $\zeta$  potential which could be attributed to a “screening effect”, reduced hydration, and protonation of the lipids in the presence of high salt concentrations. Naturally, the permanently charged quaternary ammonium derivative, TC-Chol was least affected. As a result, the reduced charge density of the lipid assemblies was severely compromised and only TC-Chol effected neutralization of DNA at charge ratios  $>2:1$ . The primary, secondary and tertiary ammonium derivatives failed to fully neutralize the negative charge of DNA in SFM, as suggested by the lack of a definitive point of electroneutrality in the laser Doppler velocimetric studies. Notably,  $\zeta$  potential values obtained under conditions of high ionic strength were characterized by a large variation of the average value most probably due to the bigger heterogeneity of the particles and weaker binding of the DNA.

We conclude that the particle size and  $\zeta$  potential measurements confirmed the formation of lipoplexes and indicated a tendency toward aggregate formation prior to the application of the active dispersions to the cell cultures. While the results obtained in the high ionic strength environment indicated the need for additional cationic lipid to neutralize the charge of plasmid DNA, the efficiency of AC-Chol and MC-Chol to effectively mediate transfection on that basis was not compromised.

**Interfacial Studies.** The assumption of these derivatives as insoluble monolayers allowed us to study them at the gas–liquid interface in order to correlate their interaction with cellular membranes. Compression isotherms of the four carbamoyl cholesterol cationic lipids were studied as a function of their molecular area at 23 and 37 °C and numerical values obtained from these isotherms are tabulated in Table 2. Compression isotherms of cationic cholesterol derivatives at room temperature were similar to those recovered at physiological temperature, signifying the lack of phase transitions within their assemblies. As methylation on the headgroup increased from the primary to the tertiary derivative, the values of the compressibility modulus  $K$  decreased from 256 to 115 mN/m and 169 to 104 mN/m at

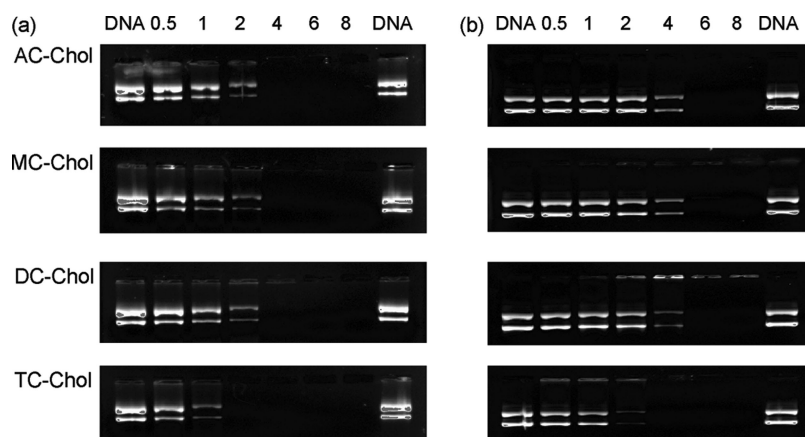


**Figure 6.** Agarose gel electrophoresis performed with AC-Chol, MC-Chol, DC-Chol, and TC-Chol at CL/DNA ratios of 0.5:1, 1:1, 2:1, 4:1, 6:1, and 8:1 (lanes 2–7). Lanes 1 and 8 contain naked DNA as a negative reference. Panel a represents CL/DNA formulations in 40 mM Tris buffer, while panel b depicts images of formulations in serum-free media.

23 and 37 °C, respectively. Further substitution on the nitrogen of the headgroup to form the quaternary ammonium salt resulted in an increased value of the compressibility modulus as compared to that of DC-Chol at ambient temperature, but exhibited a value similar to that of DC-Chol at physiological temperature. The higher stiffness observed for the ordered monolayers composed of AC-Chol, MC-Chol, and TC-Chol, is due to better hydration and efficient grafting on the water surface, while the increased hydrophobicity and poor hydration of DC-Chol resulted in increased partitioning into the gas phase and higher 2-plane elasticity of its assembled monolayers. It is plausible that the inability of DC-Chol to efficiently associate with pDNA (complexation is carried out at ambient temperature) to induce cell transfection is due to its poor interaction with the water.

**Fusion Assay.** The subtle differences in complexation and condensation between the active and nonactive cationic lipids did not reveal specific information regarding their cell surface interaction nor the endosomal release of nucleic cargo. In principle, the hydrophilicity of the cationic derivatives is related to their chemical structure and interaction with water. Conventional wisdom dictates that interaction with water should decrease as the degree of substitution of the hydrophilic headgroup increases, that is, from the primary ammonium derivative AC-Chol to the tertiary derivative DC-Chol. The pH-independent hydrophilicity of the quaternary ammonium analogue TC-Chol is expected to be higher than DC-Chol but it is not obvious how it is compared with the other two derivatives. The interfacial studies performed herein clearly indicated that DC-Chol is the most lipophilic analogue of the series, but unfortunately the experiments failed to reveal differences in hydrophilic properties among the other three analogues. Differences in particle size of cationic dispersions in physiological media (Table 1) are reflective of the differences in the physicochemical properties of these derivatives. Contrary to that, no real differences in the particle size of lipoplexes in physiological ionic strength media could be measured, especially at increasing charge

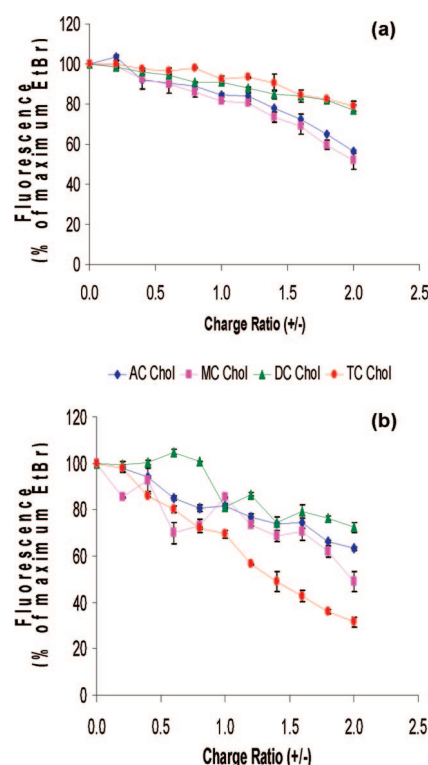


**Figure 7.** Competitive binding of cationic lipids to plasmid DNA was estimated by an ethidium bromide–DNA exclusion assay. Fluorescence values were determined as a percentage of the maximum fluorescence value obtained from a sample containing DNA and ethidium bromide in the absence of cationic lipids. The study was performed in 40 mM Tris buffer (a) and SFM (b). Data points represent the average of three experiments.

ratio. Similarly, the surface charge of all of the cationic dispersions was positive whereas that of corresponding lipoplexes was negative, with the exception of TC-Chol that exhibited a positive potential at  $+/-$  charge ratios above 2. On the basis of the similarity of the particle size and  $\zeta$  potential values of the lipoplexes, a similar interaction of the AC-Chol, MC-Chol, and DC-Chol lipoplexes and a

**Table 1.** Particle Size and  $\zeta$  Potential Measurements of Cationic Lipid Dispersions and Lipoplexes at Various CL/DNA Charge Ratios<sup>a</sup>

		Hydrodynamic Diameter (nm)		PDI <sup>d</sup>		$\zeta$ potential (mV)	
		40 mM TB <sup>b</sup>	SFM <sup>c</sup>	40 mM TB	SFM	40 mM TB	SFM
AC-Chol	lipid dispersion <sup>e</sup>	204.1	2322.0	0.24	1.0	59.01 $\pm$ 8.93	9.79 $\pm$ 19.65
	1:1	285.1	1620.5	0.25	0.33	−33.8 $\pm$ 6.9	−29.5 $\pm$ 57.2
	2:1	298.1	1331.5	0.27	0.41	−32.6 $\pm$ 8.1	−30.2 $\pm$ 56.3
	4:1	1247.7	891.2	0.33	0.22	38.1 $\pm$ 4.7	−32.6 $\pm$ 53.5
MC-Chol	lipid dispersion	169.2	1418	0.21	0.79	44.29 $\pm$ 14.76	3.77 $\pm$ 18.46
	1:1	185.4	862.3	0.24	0.3	−33.9 $\pm$ 9.9	−31.1 $\pm$ 35.2
	2:1	258.0	885.8	0.24	0.15	−33.3 $\pm$ 5.9	−31.1 $\pm$ 45.6
	4:1	782.0	877.2	0.19	0.39	41.2 $\pm$ 5.8	−30.1 $\pm$ 23.3
DC-Chol hydrochloride	lipid dispersion	209.6	182.4	0.29	0.31	34.39 $\pm$ 10.33	17.82 $\pm$ 21.74
	1:1	236.3	376.9	0.36	0.2	−35.8 $\pm$ 12.0	−32.0 $\pm$ 14.7
	2:1	250.2	417.2	0.25	0.19	−36.5 $\pm$ 11.6	−30.2 $\pm$ 11.0
	4:1	1358.7	987.1	0.80	0.35	27.7 $\pm$ 3.8	−23.9 $\pm$ 12.1
TC-Chol iodide	lipid dispersion	140.8	203.5	0.23	0.24	47.65 $\pm$ 10.93	26.23 $\pm$ 15.95
	1:1	160.4	315.9	0.21	0.18	−34.0 $\pm$ 7.6	−29.49 $\pm$ 5.97
	2:1	324.2	1467	0.29	0.2	15.0 $\pm$ 5.6	−4.9 $\pm$ 17.0
	4:1	1496.00	4446	0.99	1.0	19.34 $\pm$ 4.62	14.1 $\pm$ 13.7

<sup>a</sup> All experiments were carried out in 40 mM Tris buffer (pH 7.4) and serum free media at room temperature. Standard deviations correspond to the  $\zeta$  potential measurements and the value encompasses a positive and negative deviation. <sup>b</sup> TB denotes Tris buffer. <sup>c</sup> SFM denotes serum free media. <sup>d</sup> PDI denotes polydispersity index. <sup>e</sup> Lipid dispersions are void of DNA.

**Table 2.** Monolayer Parameters of Cholesterol-Based Cationic Derivatives Measured at the Air/Water Interphase Using 40 mM Tris Buffer pH 7.2 as the Subphase at 23 and 37 °C

	MmA ( $\text{\AA}^2$ ) at collapse		$\Pi$ (mN/m)		$K$ (mN/m)	
	23 °C	37 °C	23 °C	37 °C	23 °C	37 °C
AC-Chol( $n = 3, 2$ )	36.76 $\pm$ 0.44	38.85 $\pm$ 1.24	30.47 $\pm$ 2.31	42.37 $\pm$ 0.42	255.89 $\pm$ 59.65	168.67 $\pm$ 1.06
MC-Chol( $n = 5, 3$ )	31.80 $\pm$ 1.35	40.85 $\pm$ 1.25	38.28 $\pm$ 1.60	39.16 $\pm$ 1.02	192.42 $\pm$ 39.32	132.74 $\pm$ 6.94
DC-Chol hydrochloride( $n = 4, 7$ )	32.08 $\pm$ 1.63	33.10 $\pm$ 3.13	39.13 $\pm$ 1.10	40.58 $\pm$ 2.47	115.37 $\pm$ 18.31	104.16 $\pm$ 8.60
DC-Chol free base( $n = 5$ )	36.43 $\pm$ 0.3		39.19 $\pm$ 3.09		118.93 $\pm$ 13.76	
TC-Chol iodide( $n = 4, 4$ )	31.90 $\pm$ 0.78	32.64 $\pm$ 1.71	42.19 $\pm$ 2.49	38.76 $\pm$ 0.83	172.45 $\pm$ 18.91	101.95 $\pm$ 26.33

stronger interaction of lipoplexes composed of TC-Chol with negatively charged membranes would be anticipated.

The study proceeded in that direction to mimic the inner leaflet of the endosomal compartment using synthetic phospholipid liposomes loaded with calcein, to test the ability of each cationic derivative to lyse those vesicles by association.<sup>22–24</sup> Contrary to the expectations alluded by the particle size and  $\zeta$  potential values, similar interactions were not observed with the active and inactive analogues. AC-Chol and MC-Chol immediately ruptured the negatively charged PC/PE/PG vesicles and reached a steady state after approximately 2.5 min at  $\pm$  (CL/PG) lipid ratios of 225:1,

450:1, and 900:1 (Figure 8). The initial release rates of calcein mediated by the active lipids show a direct relationship with their patterns of cell transfection efficiency. Addition of DC-Chol and TC-Chol to the artificial vesicles resulted in a delayed small decrease of the calcein fluorescence intensity. Pertinent to our discussion above, “sticky” collisions between these two cationic lipids and the negatively charged liposomes are warranted on the basis of the positive  $\zeta$  potential values of the cationic dispersions measured in SFM (Table 1). In addition, the molar excess of the cholesterol-based cationic lipids used in this study ( $>56$ , see Materials and Methods) should be enough to destroy any bilayer structure upon partitioning. The fact that DC-Chol and TC-Chol failed to rupture the negatively charged membranes suggests that these cationic lipids are either predominantly bound to the exterior of the vesicles or their integration into the negatively charged vesicles somehow seals and stabilizes the vesicles. Contrary to that, fusion induced by the active primary and secondary derivatives suggests that dispersions formed by the active lipids have the ability to bind to the early endosomal compartment via electrostatic and hydrophobic interactions leading to

- (22) Xu, Y.; Szoka, F. C., Jr. Mechanism of DNA release from cationic liposome/DNA complexes used in cell transfection. *Biochemistry* **1996**, *35* (18), 5616–5623.
- (23) Wyman, T. B.; Nicol, F.; Zelphati, O.; Scaria, P. V.; Plank, C., Jr. Design, synthesis, and characterization of a cationic peptide that binds to nucleic acids and permeabilizes bilayers. *Biochemistry* **1997**, *36* (10), 3008–3017.
- (24) Peschka, R.; Dennehy, C.; Szoka, F. C., Jr. A simple in vitro model to study the release kinetics of liposome encapsulated material. *J. Controlled Release* **1998**, *56* (1–3), 41–51.

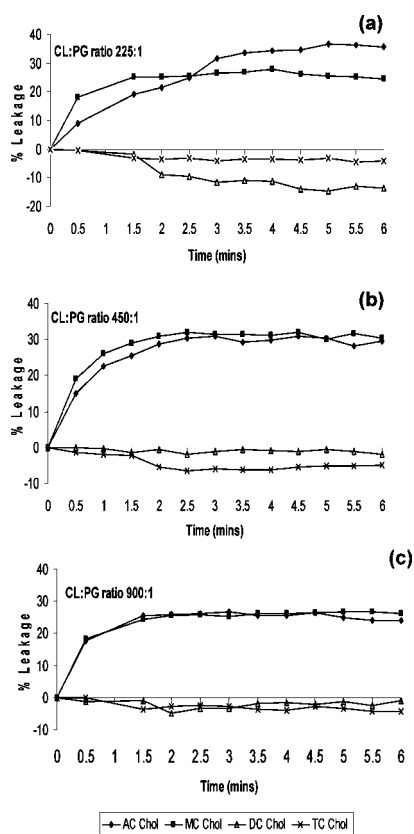


**Figure 8.** Cationic lipid-induced calcein leakage from negatively charged PC/PE/PG liposomes as a function of time.

destabilization of the endosome enabling cytosolic access to the plasmid. Apparently, the particular stereochemistry of the primary and secondary amine cationic derivatives enabled a specific interaction with phosphatidyl choline, phosphatidyl ethanolamine, and phosphatidyl glycerol that led to structural transitions of the bilayer into other types of micellar assemblies. These studies along with the minimal accumulation at the cell surface of cultured epithelial cells transfected with DC-Chol and TC-Chol (Figure 5c and d) suggest that although cell surface binding seems to occur, their cellular specificity is inadequate for the activation of uptake into an endocytotic pathway. Perhaps it is the steric hindrance introduced by the additional methyl group substitution that prevented their productive association with the naturally occurring phospholipids. It is therefore tempting to hypothesize that cell internalization of the transfection potent cationic lipids, is the result of their binding to cell surface proteoglycans followed by a structure specific interaction with the natural phospholipids of the cell membranes, leading to endocytotic events and subsequent endosomal release into the cytosol.

## Conclusion

The results of this study emphasize that although the physicochemical properties and the interaction with DNA of all four analogues were similar, their cellular interaction varied dramatically, suggesting that cell surface specificity and intracellular navigation were the limiting steps in mediating transfection by the novel active derivatives, AC-Chol and MC-Chol. The biological specificity displayed here is directly attributed to a structure specific interaction with the cell surface given that all the experiments were performed in the absence of a helper lipid. The specific location of the internalized lipoplexes is presumably the endosomal compartment based on previous endocytic and trafficking studies and is supported by the fusion experiments in this investigation.<sup>12,14,15,25</sup> This conclusion follows from the small differences in the physical characteristics of all four carbamoyl cholesterol derivatives compared with the conspicuous differences illustrated by the biological studies. Biological specificity of AC-Chol and MC-Chol imparted an increased fluorescence as a result of calcein release when applied to artificial liposomal vesicles together with their ability to gain entry into the cell as indicated by transfection experiments using fluorescently labeled DNA. The primary and secondary cholesterol derivatives that have been synthesized are able to overcome two widely accepted cellular barriers to efficient gene transfer, namely (1) lipoplex-cell surface interaction leading to internalization of the lipoplex, and (2) release of encapsulated genetic DNA into the cytoplasm. That accomplishment was preceded by their ability to efficiently associate with DNA and mediate moderate DNA compaction.

While progress continues to occur in the development of efficient cholesterol cationic nonviral gene delivery vectors further investigations need to be carried out with respect to their uptake by a specific endocytotic pathway and their intracellular mediation of nucleic acid release. Such studies will enhance their potential use as effective nonviral vectors in achieving gene delivery.

**Acknowledgment.** This work was supported in part by a grant from the National Institutes of Health, EB004863, and the Arnold and Marie Schwartz College of Pharmacy and Health Sciences.

MP700131C

- (25) Ruponen, M.; Ronkko, S.; Honkakoski, P.; Pelkonen, J.; Tammi, M.; Urtti, A. Extracellular glycosaminoglycans modify cellular trafficking of lipoplexes and polyplexes. *J. Biol. Chem.* **2001**, 276 (36), 33875–33880.